Optimization of Algae Residues Gasification: Experimental and Theoretical Approaches

Optimization of Algae Residues Gasification: Experimental and Theoretical Approaches

M.S.N. Atikah[1], Taufiq Yap Y.H.[2], R.A. Ilyas[3], Razif Harun[1],*

[1]Department of Chemical and Environmental Engineering, Faculty of Engineering, Universiti Putra Malaysia, 43400 UPM Serdang, Selangor, Malaysia.
[2]Chancellery Office, Universiti Malaysia Sabah, Kota Kinabalu, Sabah 88400, Malaysia
[3]School of Chemical and Energy Engineering, Faculty of Engineering, Universiti Teknologi Malaysia

E-mail: mh_razif@upm.edu.my

Abstract. Gasification is one of the thermochemical pathways of biomass conversion that produces synthesis gas, tar, and char. This study aims to convert algal residues via gasification at different operating conditions; temperature, equivalence ratio, and biomass loading. The study was carried out in 3 steps; (1) testing the outcomes of temperature and loading effects on synthesis gas yield, (2) experimental optimization of gasification via Design Expert, and (3) theoretical optimization of gasification via Aspen Plus simulation. Temperature and equivalence ratio highly influenced synthesis gas composition, while loading demonstrated less effect on the synthesis gas composition. The experimental and simulated gasification outcomes were compared to obtain optimized conditions that produce high H_2 and CO yields. The data were validated using root mean square error. The optimized temperature, loading, and equivalence ratio were found for both algal residues that produced 36.38 and 13.28mol% of H_2 and CO, respectively for lipid extracted algae (LEA) and 47.99 and 26.05mol% of H_2 and CO, respectively for fucoidan extracted seaweeds (FEA). There was a considerable variation between experimental and simulated data due to the simulation and experimental limitations. The average Carbon Conversion Efficiency values were 66.36 and 80.42% for LEA and FES, respectively, denoting that LEA produced less carbon-containing products, while FES produced more carbon-containing products. In conclusion, LEA gasification yielded more H_2 while FEA produced more CO.

1. Introduction

Biomass is one of the renewable energy sources categorized into first-, second-, and third-generation renewable biofuels that are developed to achieve the same objective; towards minimizing the reliance upon fossil fuels resources. Algal biofuels or third-generation biofuels are algae-based biofuels products introduced to improve the limitations of the first and second-generation biofuels, e.g., food versus fuel, and colossal land and extensive fertilizer use (Bowyer et al., 2018; Prakash et al., 2014). These biofuels manufacturing produces by-products known as lipid-extracted algae (LEA) that is still rich in carbohydrate, protein, and a fraction of un-extracted lipid (Maurya et al., 2015). With the utilization of the LEA, the efficiency of this crucial part of algae to fuel processing is expected to increase since the lipid extraction itself is an expensive process (Chen et al., 2012; Ranjith Kumar et al., 2015). Although

microalgal gasification has been extensively studied by researchers at various operating conditions for different algae species to yield high-quality fuel (Nurdiawati et al. 2018; Ebadi et al. 2017; Raheem et al. 2018), few works are reported in LEA gasification.

On the other hand, macroalgae or seaweeds are widely used in food and health supplement production since they are rich with bioactive compounds that are proven to have antioxidant properties (Meillisa et al., 2013). Seaweeds are utilized for fucoidan, fucoxanthin, polyphenol, isoflavones, phenol, polysaccharides, and lipids (Roh et al., 2008). Extraction of the bioactive compounds will produce extracted algal residue that still contains compounds other than the extracted ones. This algal residue will be addressed as FES in the latter part of this paper.

Optimization studies were performed experimentally and theoretically in Design Expert 7.7 software and Aspen Plus V8.8 software, respectively. Experimental optimization aims to find the optimized conditions for high syngas yield, focusing on H_2 and CO yields. Theoretical optimization verified the validity of the experimental data based on the simulated gasification process performed at similar conditions as the gasification experiments. Both optimization studies are crucial in determining optimum syngas yield and theoretical syngas yield at specific process parameters. The air gasification process was simulated in Aspen Plus V8.8 software. This software has been used for modeling, simulation, optimization, sensitivity analysis, and economic evaluation of chemical processes (Sun, 2014).

However, little works have been reported utilizing algal residues from the lipid and fucoidan extraction processes for synthesis gas production. This study aims to find the optimized conditions of LEA and FES conversion to synthesis gas via a conventional air gasification process. This creates an alternative path of applying algae residues for synthesis gas production that solves the underutilization issue of the algal residues and makes the overall algal processing more economically and environmentally sustainable. To the best of our knowledge, few Aspen Plus gasification modeling were carried out on algal residue, and none of the literature reported on the fixed bed air gasification of algal residue; hence, this study builds a gasification model for LEA and FES that is reproducible for gasification of other algal residues.

2. Materials and methods

2.1 Materials

The lipid extracted algae, LEA, was obtained from the subcritical water lipid extraction method of *Nannochloropsis gaditana* biomass; meanwhile, the fucoidan extracted seaweeds, FES is the mixture of seaweeds residue (*Sargassum sp*., *Padina sp*., and *Enteromorpha sp*.) from subcritical water fucoidan extraction. Both LEA and FES were dried in an oven at 105℃ for 48h prior to crushing in mortar and pestle. Both solid residues were then sieved to 300 μm size and separately kept in air-tight containers prior to gasification.

2.2 Gasification

The gasification process was carried out in a Temperature Program Gasifier (TPG) (model: VSTF50/150-1100, 1.2kW/6A) (Figure 1). The reactor was connected to a digital gas flowmeter (model: FMA5506A; Omega Engineering, Inc.) that detected gas flow in the 0-50 mL/min range. Both LEA and FES were heated inside the furnace at experimental parameter variations based on the experimental runs, as detailed in Table 1. The gasifying medium used was compressed air supplied by a gas cylinder. Moisture was trapped in a moisture trap filled with cotton wool prior to cooling down by immersing the gas tube in an ice bath before the gas collection in a 1L Tedlar gas bag. This step ensured that the gas collected was at room temperature and moisture-free. All gasification processes were performed at 30 minutes holding time to allow for stable temperature and complete reaction in the gasifier. Upon completion of the 30 minutes holding time, the furnace was let to cool back to room temperature.

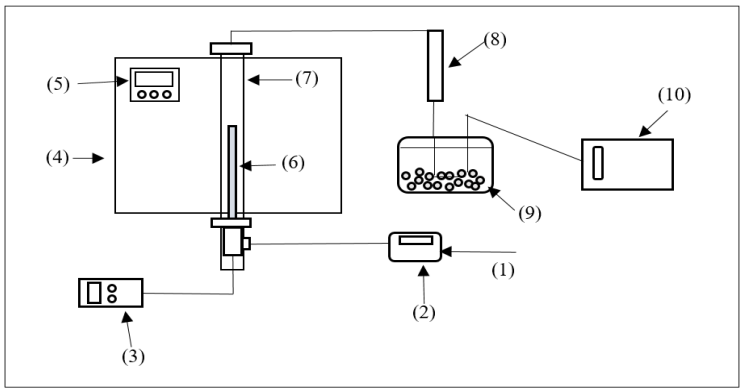

Figure 1. Schematic diagram of the Temperature Program Gasifier (TPG) setup (1) compressed air from the gas cylinder; (2) air flowmeter; (3) thermocouple controller; (4) electric furnace; (5) furnace controller; (6) thermocouple; (7) stainless steel reactor tube; (8) moisture trap; (9) ice bath; (10) gas collection bag.

The heating rate, holding time, and equivalence ratio (ER) were maintained at 20 ^{o}C/min, 30 min, and 0.25, respectively. The experimental design for the gasification at different process parameters was performed in Design Expert 7.0 software using response surface via central composite design (CCD) approach, aiming to find the optimized conditions for high syngas yield. This approach was used to determine the number of experiments to be evaluated to optimize the variables and responses. Table 1 shows the parameters involved in this study and the level of the parameters, meanwhile Table 2 displays the optimization of gasification experiments generated based on the parameters and their levels. The ranges of parameters for optimization gasification experiments, namely the temperature, loading, and ER values, were determined from the preliminary experiments based on the range of parameters that produced high H_2 and CO yields.

Table 1. Experimental parameters involved in this study and their levels in the central composite design (CCD) approach.

Parameters	Level				
	-2	-1	0	+1	+2
Temperature (^{o}C)	600	700	800	900	1000
Loading (g)	0.3	0.4	0.5	0.6	0.7
ER value	0.1	0.2	03	0.4	0.5

Table 2. List of optimization gasification experiments using central composite design (CCD) approach. Each run was carried out in duplicate.

Run	Temperature	Loading	ER
1.	(0)	(0)	(0)
2.	(+1)	(+1)	(+1)
3.	(+2)	(0)	(0)
4.	(+1)	(+1)	(-1)
5.	(0)	(-2)	(0)
6.	(0)	(+2)	(0)
7.	(-1)	(+1)	(+1)
8.	(+1)	(-1)	(-1)
9.	(-1)	(+1)	(-1)
10	(-2)	(0)	(0)
11.	(+1)	(-1)	(+1)

12.	(-1)	(-1)	(+1)
13.	(0)	(0)	(-2)
14.	(-1)	(-1)	(-1)
15.	(0)	(0)	(+2)
16.	(0)	(0)	(0)
17.	(0)	(0)	(0)

2.3 Gas analysis

A Gas Chromatography with Flame Ionization Detector (GC-FID) (Agilent Technologies, 6890 N) was used in the syngas analysis to study the molar composition of desired gases; hydrogen (H_2), carbon monoxide (CO), carbon dioxide (CO_2), and methane (CH_4) contained in the syngas. Analysis of the syngas of each syngas sample was carried out according to ASTM Method D3612-96. The sample gas was injected into a 30 m × 0.53 mm Carboxen-1010 PLOT column. The oven was set at 350°C, and argon gas was used as carrier gas under 3.0 mL/min flow. The presence and composition of H_2, CO, CO_2, and CH_4 were analyzed from the chromatogram generated from GC-FID in parts per million (ppm) unit. The mole of each gas generated from the chromatogram was calculated by using equation (1) below:

$$mol = \frac{Area\ of\ individual\ gas\ (in\ chromatogram)}{Standard\ calibrated\ area\ of\ gas} \times Standard\ gas\ mole \quad (1)$$

Next, the mole percent of each gas was evaluated from equation (2):

$$mol\ \% = \frac{mol\ of\ individual\ gas}{total\ mol\ of\ gas\ mixture} \times 100 \quad (2)$$

2.4 Aspen Plus simulation

The model comprises three main stages, drying, pyrolysis, and gasification. Table 3 shows the list of components used in the simulation model. The enthalpy and density of both non-conventional components in Table 3 are HCOALGEN and DCOALIGT, respectively. Each stage was modeled using a different type of reactor that connected to materials streams, as summarized in Tables 4 and 5. Aspen Plus flowsheet for the model is shown in Figure 2. From Table 4, LEA and FES drying was not considered a chemical reaction. However, RStoic block converted portions of LEA and FES into moisture, which were 4.12 and 5.29wt%, respectively, based on moisture contents of both algae residues from proximate analysis data. The equation in Table 4 indicated that 1 mole (1 lb) of biomass was converted into 0.0555084 mole (1lb) of water since Aspen Plus treated all NC having a molecular weight of 1.0. The volume flow rate of air used in the drying of the LEA and FES was fixed at 100 L/h, in which the involvement of air at this stage did not affect the ER value, whereby the volume of air required for all gasification runs was higher than this value. Hence, the volume of air that entered the COMBUST unit was subtracted by 100 L/h from the actual values.

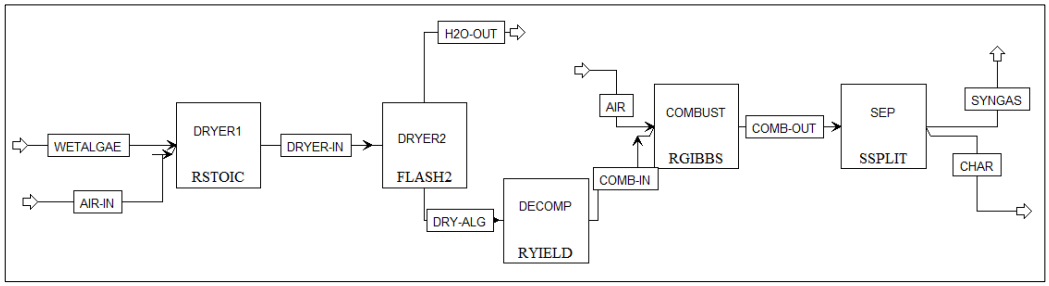

Figure 2. Aspen Plus flowsheet of the gasifier model.

Table 3. List of components in the simulation model.

Component ID	Type	Component name	Formula
Biomass	Non-conventional	-	-
C	Solid	Carbon-graphite	C
H_2	Conventional	Hydrogen	H_2
N_2	Conventional	Nitrogen	N_2
O_2	Conventional	Oxygen	O_2
S	Conventional	Sulphur	S
CO	Conventional	Carbon monoxide	CO
CO_2	Conventional	Carbon dioxide	CO_2
CH_4	Conventional	Methane	CH_4
H_2O	Conventional	Water	H_2O
ASH	Non-conventional	-	-

Table 4. Aspen Plus unit operation models description.

Process	Aspen Plus block/ID	Description	Process input
Drying	RStoic/ DRYER1	● Drying of biomass by removing biomass moisture. ● RStoic is chosen due to known stoichiometry of the process.	● Pressure 1 atm, heat duty 0 kJ/hr, isobaric and adiabatic, reaction occurred; $biomass \rightarrow 0.0555084 H_2O$.
Water separation	Flash2/ DRYER2	● RStoic and flash drum simulate drying and removal of water from the biomass as a single block.	Pressure 1 atm, heat duty 0 kJ/hr, isobaric and adiabatic, valid phases are vapor-liquid.
Pyrolysis	RYield/ DECOMP	● Conversion of NC components in the biomass to conventional components using FORTRAN statement (calculator block).	Temperature 500 ^oC, pressure 1 atm, C, H_2, N_2, O_2, S, and ash are the yields
Gasification	RGibbs/ COMBUST	● Simulation of solid-gas reactions.	Pressure 1 atm, temperature (600-1000 ^oC).
Char separation	SSplit/ SEP	Separation of gasification products to syngas and char.	Syngas stream, MIXED substream was set to 1. For char stream, CIPSD and NCPSD were set to 1.

NC= non-conventional, FORTRAN= formula translation.

Table 5. Materials streams description.

Stream name	Description	Process input
WETALGAE	Introduction of wet biomass containing moisture.	Mass flow rate (100-1000 kg/h), proximate and ultimate analysis of biomass.
AIR-IN	Air used in the drying of the biomass.	Volumetric flow rate fixed to 100 L/h.
DRYER-IN	Wet biomass into water separator.	-
H2O-OUT	Water vapour from biomass drying.	-

DRY-ALG	Dried biomass from biomass drying, into pyrolysis stage.	-
COMB-IN	Products from pyrolysis, into gasification reactor.	-
AIR	Air needed for gasification process, volume determined by equivalence ratio (ER) value.	Volume of air varies to meet desired ER values.
COMB-OUT	Mixture of products from gasification process.	-
SYNGAS	Synthesis gas from the whole process.	-
CHAR	Solid residue from overall process.	-

The RYield (DECOMP) block simulated decomposition or pyrolysis process that occurred at a temperature lower than 500℃, producing combustible gases and solid carbon. This block input required yield of the process in mole fraction; hence, they were assumed as 0.2, 0.2, 0.2, 0.1, 0.1, 0.1, 0.1 moles, respectively, for C, H_2, H_2O, N_2, O_2, S, and ash to give the total mole fraction of the yields to be 1. The output mole fraction yields were corrected by the calculator block installed before the RYield (DECOMP) block to calculate the exact yield of the pyrolysis process. The results generated in Aspen Plus for the COMB-IN (COMBUST block inlet) stream were based on the actual yield as evaluated by the calculator. The calculator specifications are shown in Tables 6 and 7 (Aspentech, 2013).

Table 6. Calculator specifications for pyrolysis block using category: streams.

Variable name	Type	Stream	Substream	Component	Attribute	Elements
ULT	Compattr-Vec	DRY-BIO	NCPSD	BIOMASS	ULTANAL	
WATER	Compattr-Var	DRY-BIO	NCPSD	BIOMASS	PROXANAL	1

Table 7. Calculator specifications for pyrolysis block using category: block.

Variable name		ID1	ID2
H_2O	Type: Block-var, Block: DECOMP, Variable: MASS-YIELD	H_2O	MIXED
ASH		ASH	NCPSD
CARB		CARB	CIPSD
H_2		H_2	MIXED
N_2		N_2	MIXED
O_2		O_2	MIXED
S		S	MIXED

The FORTRAN statement for the calculator block was entered as below:

```
FACT = (100 - WATER) / 100
H2O = WATER / 100
ASH = ULT(1) / 100 * FACT
CARB = ULT(2) / 100 * FACT
H2 = ULT(3) / 100 * FACT
N2 = ULT(4) / 100 * FACT
O2 = ULT(5) / 100 * FACT
SULF = ULT(6) / 100 * FACT
```

The calculator block was set to execute before unit operation DECOMP. The simulation was performed according to experimental conditions to produce comparable results. In RGibbs block, the reactor identified all components as products in the mixed-phase. Carbon was set as pure solid coming from the gasification process known as ash at the end of the process and was separated from the syngas in the SSplit (SEP) block. RGibbs (COMBUST) block was used in the simulation of the gasification phase as reported in Cohce et al. (2011) for biomass gasification, wood gasification in Lestinsky and Palit (2016a), and bamboo gasification (Chen et al., 2014).

Aspen Plus sensitivity analysis tool was used in the study of the effects of temperature and loading on the syngas composition. This tool analyzed the effect of varying process parameters on the desired output, or in this study, the effects of varying temperature (600-1000℃) with 10℃ increment and loading (300-700 kg) with 10 kg increment syngas composition. The sensitivity analyses were run at COMBUST block for gasification temperature and WETALGAE stream for algae residues loading. Table 8 shows the input parameters of the temperature and biomass loading. The outputs from the simulation were plotted as parameters (temperature and loading) against syngas compositions (H_2 and CO).

Table 8. GASIF block specifications.

Variable	Type	Block/stream	Variable	Unit	Limits	Increment
Temperature	Block-var	COMBUST	TEMP	℃	600-1000	10
Biomass loading	Stream-var	WETALGAE	MASS-FLOW	kg	300-700	10

The development of this gasification model was based on a few assumptions to simplify the calculations made as follows (Mutlu & Zeng, 2020; Panda, 2012; Rosha et al., 2021):

1. The LEA and FES particles were assumed to be spherical in shape and have a uniform size, which was 300 microns.
2. The gasifier was assumed to operate isothermally at a steady-state; hence, heat loss from the gasifier was neglected, and the temperature inside the gasifier was uniform.
3. The gasifier was operated at atmospheric pressure (1 atm); therefore, no pressure drop occurred in the gasifier.
4. The products of the gasification, which were oxides of nitrogen and sulfur, were neglected since nitrogen and sulfur were present in a very small percent on a dry weight basis, less than 1%.
5. The gas phase was assumed to be instantaneous and was perfectly mixed with the solid phase.
6. The volatile products formed from the reactions are H_2, CO, CO_2, CH_4, and H_2O.
7. Char, the solid product from the gasification, only consisted of black solid carbon and ash.

2.5 Data validation

Data validation for experimental and Aspen Plus optimization was performed using root mean square error (RMSE) value that was calculated using equation (3):

$$RMSE = \sqrt{\frac{\sum_{i=1}^{N}(y_{predicted} - y_{experimental})^2}{N}} \quad (3)$$

where N is a number of sets, which was 17, $y_{predicted}$ was predicted values in Aspen Plus, and $y_{experimental}$ was experimental data. RMSE shows the error between the mean values of the predicted and experimental data. The data are said to be in good agreement when the RMSE is less than 0.5 (Veerasamy et al., 2011).

2.6 Carbon conversion efficiency (CCE)

CCE was determined via the elemental balance method that was calculated by using equation (4):

$$CCE = \frac{total\ carbon\ output}{total\ carbon\ input} \times 100\% \quad (4)$$

where total carbon output=total mole of carbon in the producer gas, total carbon input=total mole of carbon in the LEA and FES.

3. Results and discussion

3.1. Gasification of LEA and FES

The gasification experiments for both residues were carried out in a Temperature Program Gasifier (TPG) by varying temperature and biomass loading. The simulation of the gasification process was also performed using Aspen Plus software to compare the experimental findings with the theoretical prediction.

3.1.1 Effect of temperature. The gasification temperatures used in this study were in a range of (600-1000 ℃) with 100 ℃ increments. The biomass loading and ER were kept constant at 0.4 g and 0.25, respectively. LEA and FES gasification is an endothermic process that requires the supply of heat to shift the gasification reactions to the right. All endothermic processes that occurred during gasification were favored as the temperature went higher. It was found that the H_2 was increased as the temperature was increased, as shown in Table 9. The highest H_2 composition was 51.2 mol % at 700 ℃; meanwhile, CO yield was the highest at 1000℃, which was 54.4 mol% for LEA from the experiment. Slightly different values of 51.85 mol% H_2 and 48.01 mol% CO were obtained with the simulated results, as observed in Table 10. However, H_2 yields were decreased to 48.5 and 50.38 mol% at 800℃ for the experimental and predicted H_2 yields, respectively, suggesting that 700ºC is the optimum temperature for H_2 production by varying only the temperature.

Table 9. Effect of temperature and loading in gasification of LEA and FEA. The results presented are average values from 2 replicates.

				Syngas composition		(mol %)	
	Experimental parameters			LEA		FEA	
	Temp (ºC)	Loading (g)	ER	H_2	CO	H_2	CO
Effect of temperature	600	0.4	0.25	47.8±0.2	20.1±0.9	46.2±0.9	16.3±0.7
	700	0.4	0.25	51.2±0.8	33.3±0.7	53.3±0.7	25.3±0.5
	800	0.4	0.25	48.5±0.5	46.2±0.8	42.8±0.2	40.6±0.4
	900	0.4	0.25	45.6±0.4	49.6±0.4	40.6±0.4	45.5±0.5
	1000	0.4	0.25	40.7±0.3	54.4±0.6	38.5±1.0	50.7±1.3
Effect of loading	700	0.3	0.25	28.3±0.7	16.4±0.6	13.8±0.6	11.4±0.4
	700	0.4	0.25	33.1 ±0.9	14.3±0.7	18.2±0.8	10.7±0.8
	700	0.5	0.25	45.6±0.4	5.0±0.8	25.5±0.5	9.5±1.0
	700	0.6	0.25	47.0±1.2	4.6±0.4	46.1±1.3	6.9±0.6
	700	0.7	0.25	50.6 ±0.4	2.9±0.3	48.2±0.9	5.5±0.5

Table 10. Aspen Plus simulation data for effect of temperature and loading of LEA and FEA gasification.

				Syngas composition		(mol %)	
	Process parameters			LEA		FEA	
	Temp (°C)	Loading (g)	ER	H_2	CO	H_2	CO
Effect of temperature	600	0.4	0.25	51.75	18.10	34.03	18.20
	700	0.4	0.25	51.85	35.91	40.82	25.61
	800	0.4	0.25	50.38	46.21	42.68	25.21
	900	0.4	0.25	50.79	47.71	46.22	26.26
	1000	0.4	0.25	50.86	48.01	53.26	29.30
Effect of loading	700	300	0.25	51.85	35.91	14.19	19.66
	700	400	0.25	51.90	35.87	22.53	11.37
	700	500	0.25	51.92	35.84	27.91	8.36
	700	600	0.25	51.94	35.83	36.41	6.31
	700	700	0.25	51.96	35.81	39.06	6.89

This can be explained by the minimal impact of the water-gas-shift reaction ($CO + H_2O \leftrightarrow H_2 + CO_2$) that resulted in the consumption of both H_2 and CO_2 and boosted production of CO (Chen et al., 2008). In addition, major gases obtained were H_2 and CO from both experimental and predicted values, which indicated that major reactions involved in the gasification were oxidation, water-gas, and water-gas-shift reactions (Sanchez-Silva et al., 2013). There were variations in the compositions of H_2 and CO obtained experimentally and theoretically, whereby the predicted H_2 from Aspen Plus was higher than the obtained H_2 and vice versa for CO.

Moreover, a consistent trend was observed for FES. Around 53.3 and 50.7 mol% of H_2 and CO were found at 700 and 1000 °C, respectively. These values were higher than the predicted composition of H_2 and CO obtained at the same process parameters. However, H_2 yield was dropped to 44.8 mol% at 800 °C. Bouduard reaction, an endothermic reaction, also contributed to the increase in CO compositions due to the CO_2 reaction with char to produce CO (Doherty et al., 2009). This resulted in an increment of CO with temperature.

A significant difference in the experimental syngas composition and the ones obtained from the Aspen Plus simulation was observed. However, the trends of the changes in the syngas compositions were similar. This might be contributed by the limitations of the experimental facilities, whereby the gasifier was not properly insulated, which caused heat loss from the system. In addition, the Aspen Plus simulation excluded the heating rate and duration of the gasification process in the simulation. Overall, the experimental and predicted parameters that yielded the highest H_2 and CO were similar despite the variance between the experimental and predicted compositions of the syngas.

3.1.2 Effect of Loading. The effect of loading was investigated by manipulating biomass loading (0.3, 0.4, 0.5, 0.6, and 0.7 g) while temperature and ER were kept constant at 700 °C and 0.25, respectively. Table 9 shows the H_2 yield was increased from 28.3 to 50.6 mol% as the LEA loading was increased from 0.3 g to 0.7 g due to the occurrence of water-gas shift reaction, methanation reaction, and dry reforming reaction (Doherty et al., 2009; Raheem et al., 2015). As for the predicted values, 2.34 mol% was obtained at 0.3 g and 0.4 g and increased to 2.37 mol% at 0.7 g. However, the increments of the yields in the predicted compositions from Aspen Plus were smaller than that from experimental values. Raheem et al. 2015c reported that the increasing ratio of biomass improved the yield of H_2 and CH_4 in the syngas, as well as the total carbon conversion and gasification efficiency. CO yield was decreased as the loading was increased, which was from 16.4 mol% to 2.9 mol%. This was due to enhancing the water-gas-shift reaction at higher loading that promoted H_2 and suppressed CO production. Aspen Plus prediction also resulted in a similar pattern of CO yield; however, the decrement occurred in a smaller range than the experimental results.

FES exhibited the same trend of syngas compositions as LEA. H_2 yield was increased from 14.19 mol% at 0.3 g to 39.06 mol% at 0.7 g. CO was decreased from 19.66 to 6.89 mol% with increasing FES loading. Unlike the experimental findings, the syngas composition from the simulation did not significantly affected by the variance of the loading due to the fact that loading did not directly involve the water-gas shift, methanation, and dry reforming reaction mechanisms. Hence, the huge variance of syngas compositions yields from the experiment compared to the simulation might be contributed by the huge effect of the water-gas shift, methanation, and dry reforming reactions. In addition, the difference also was contributed by the limitations of the experimental facilities and limitations of Aspen Plus simulation.

3.2 Experimental optimization

Experimental optimization of gasification via central composite design (CCD) approach was carried out, and the findings are presented in Table 11. The H_2 was the dominant gas found in both LEA and FES, produced in the range of 28.24-45.31 mol% for LEA and 26.48-38.02 mol% for FES, respectively. The highest H_2 yield was found at 900℃, 0.4 g loading, and ER of 0.4, while the lowest yield was at 600℃, 0.5 g loading, and ER of 0.3 for both algae residues.

Table 11. Experimental optimization data using Central Composite Design (CCD) approach.

Run	Process parameters			Syngas compositions (mol %)			
				LEA		FEA	
	Temperature	Loading	ER	H_2	CO	H_2	CO
1.	800 (0)	0.5 (0)	0.3 (0)	41.63	12.34	35.68	21.56
2.	900 (+1)	0.6 (+1)	0.4 (+1)	38.58	19.92	38.02	23.81
3.	1000 (+2)	0.5 (0)	0.3 (0)	43.88	20.98	38.19	31.00
4.	900 (+1)	0.6 (+1)	0.2 (-1)	42.61	18.00	36.67	28.08
5.	800 (0)	0.3 (-2)	0.3 (0)	43.64	12.52	34.76	25.04
6.	800 (0)	0.7 (+2)	0.3 (0)	42.13	12.89	35.15	22.98
7.	700 (-1)	0.6 (+1)	0.4 (+1)	37.36	9.75	35.73	18.69
8.	900 (+1)	0.4 (-1)	0.2 (-1)	41.31	17.48	38.97	27.39
9.	700 (-1)	0.6 (+1)	0.2 (-1)	30.51	13.31	31.31	20.15
10	600 (-2)	0.5 (0)	0.3 (0)	28.24	12.01	26.48	19.60
11.	900 (+1)	0.4(-1)	0.4 (+1)	45.31	12.97	37.09	27.86
12.	700 (-1)	0.4 (-1)	0.4 (+1)	41.62	6.30	31.65	19.38
13.	800 (0)	0.5 (0)	0.1 (-2)	35.48	16.02	37.17	23.07
14.	700 (-1)	0.4 (-1)	0.4 (-1)	30.50	15.67	32.53	21.36
15.	800 (0)	0.5 (0)	0.5 (+2)	41.77	12.91	37.27	20.91
16.	800 (0)	0.5 (0)	0.3 (0)	38.37	15.48	34.16	20.85
17.	800 (0)	0.5 (0)	0.3 (0)	41.34	13.99	36.36	22.56

ER= equivalence ratio.

The maximum CO yields were obtained at 1000℃, 0.5 g loading, and ER of 0.3 for both algae residues, 20.98 mol% for LEA, and 31.00 mol% for FES, respectively. The conditions that produced the highest yield of H_2 and CO were found at the same temperature, loading, and ER value for both algal residues. However, the compositions of the gases were different, where LEA produced more H_2 and less CO compared to FES. The variations in the experimental optimization data revealed that the changes in experimental parameters (temperature, loading, and ER) affected the syngas compositions.

The study of H_2 production revealed that the yield was increased with the increase of temperature and loading and decreased with increasing ER value. Maximum yield was found in the range of temperature of 800-1000℃, loading of 0.3-0.5 g, and ER of 0.1-0.3. The equilibrium of the steam reforming reaction ($CH_4 + CO_2 \leftrightarrow 2CO + 2H_2$) and the water-gas-shift reaction ($CO + H_2O \leftrightarrow H_2 + CO_2$)

was shifted to the right at higher loading due to the increment in the mass of reactive species per unit volume (Raheem et al., 2015). CO yield was found at a maximum at 900-1000℃ as a result of the water-gas-shift reaction at higher temperatures and loadings. Steam reforming reaction suppressed CO_2 production at higher temperatures by promoting CO production. As the ER value was increased, higher oxygen that acted as an oxidant was supplied to the system. Hence, H_2 and CO yields were decreased due to the enhancement of the oxidation process that promoted CO_2 production ($C + O_2 \leftrightarrow CO_2$) (Raheem et al., 2015).

For FES, the yield of H_2 was maximum in the range of 650-800℃ and ER 0.1-0.45; meanwhile, FES loading did not significantly affect the H_2 yield. A similar phenomenon occurred for CO, as the yield was only significantly affected by temperature and ER. CO was found to increase with temperature and decrease with ER increment, whereby the maximum yield was found at 900-1000℃ at lower ER value. FES loading also did not significantly affect H_2 and CO compositions since it was not involved in the gasification mechanism, as revealed by H_2 and CO.

Analysis of variance (ANOVA) was performed in Design Expert 7.0 software to study the significance of the change in process parameters (temperature, loading, and ER value) to syngas compositions from *p*-value at 95% confidence level. The *p*-value is used to determine the probability of obtaining predicted data closer to experimental data; thus, *p*-value<0.05 indicates the model is significant.

Table 12 and Table 13 show that regression coefficient (R^2) and adjusted regression coefficient (Adj-R^2) values for all compositions were above 0.75, which indicated the aptness of the model. Hence, the quadratic models are valid interpretations of the experimental data.

Table 12. Analysis of variance (ANOVA) for syngas composition for LEA.

	H_2 (mol %)			CO (mol %)		
Variable	SS	DF	P	SS	DF	P
A	214.49	1	0.00	108.02	1	0.00
A×A	32.30	1	0.01	7.40	1	0.08
B	10.93	1	0.07	6.20	1	0.10
B×B	5.85	1	0.16	3.14	1	0.00
C	59.55	1	0.00	31.59	1	0.00
C×C	6.96	1	0.13	0.10	1	0.00
A×B	0.17	1	0.79	5.06	1	0.13
A×C	40.50	1	0.00	13.42	1	0.03
B×C	18.91	1	0.03	18.73	1	0.01
error	16.51	7		12.25	7	
Total	415.92	16		209.95	16	
R^2	0.96			0.94		
Adj-R^2	0.91			0.87		

SS: Sum of squares; DF: Degree of freedom.

Table 13. Analysis of variance (ANOVA) for syngas composition for FEA.

	H_2 (mol %)			CO (mol %)		
Variable	SS	DF	P	SS	DF	P
A	84.89	1	0.00	158.76	1	0.00
A×A	20.56	1	0.01	14.94	1	0.00
B	0.47	1	0.46	5.57	1	0.04
B×B	0.13	1	0.70	5.73	1	0.04
C	0.17	1	0.66	8.66	1	0.02
C×C	0.27	1	0.58	0.00	1	0.99
A×B	0.19	1	0.64	0.27	1	0.60

A×C	1.07	1	0.28	0.016	1	0.89
B×C	2.50	1	0.12	2.23	1	0.15
error	5.48	7		6.11	7	
Total	118.70	16		200.64	16	
R^2	0.95			0.97		
Adj-R^2	0.89			0.93		

SS: Sum of squares; DF: Degree of freedom.

The polynomial model equations and the predicted optimized gasification conditions of both residues are displayed in Table 13 and Table 14. The model equation can be used to calculate the optimized yield of H_2, CO, CO_2, and CH_4, as detailed in Table 14 and Table 15. The optimum H_2 yield from LEA was found to be higher than FES, which were 49.81 mol% at 849.77 ℃, loading of 0.3 g, and ER value of 0.4, and 47.54 mol% at 743.47℃, loading of 0.65 g an ER value of 0.15, respectively.

Table 14. Polynomial model equations built from the CCD approach and the optimized conditions for LEA gasification.

Response variables (mol%)	Polynomial model equations	Optimum conditions
H_2	-173.37103 + 0.38534 A - 23.04961 B + 324.90917 C - 0.014750 AB - 0.225 AC - 153.75 BC - 1.69273E-4 A^2 + 72.02708 B^2 - 78.58667 C^2.	A=849.77℃, B=0.3 g, C=0.4, Yield=49.81 mol%.
CO	118.0125 - 0.1802 A – 49.986 B - 200.9786 C + 0.0795 AB + 0.1295 AC + 153 BC +8.10443E-005 A^2 - 52.77564 B^2 +9.44976 C^2.	A=900.88℃, B=0.64 g, C=0.42, Yield=21.17 mol%.

Table 15. Polynomial model equations built from the CCD approach and the optimized conditions for FEA gasification.

Response variables (mol%)	Polynomial model equations	Optimum conditions
H_2	-24.63371 + 0.18787 A + 16.60191 B +6.76598 C - 0.015375 AB + 0.036625 AC - 55.875 BC - 1.35060E-4 A^2 + 10.60372 B^2 - 15.38245C^2.	A=743.47℃, B=0.65 g, C=0.15, Yield=47.54 mol%.
CO	75.19104 - 0.13962 A - 47.24499 B + 22.09536 C - 0.018250 AB - 4.5E-3 AC -52.75 BC + 1.15122E-004 A^2 + 71.28163 B^2 -0.13616C^2.	A=961.23℃, B=0.36 g, C=0.1, Yield=33.10 mol%.

Table 16 presents the optimized conditions for syngas production from gasification from this study and the literature. Steam gasification conducted by Onwudili et al. (2013) produced the least amount of H_2 compared to conventional air gasification in this study and that of Raheem et al. (2015c). The optimized temperatures found in all studies were lower than 800℃, which proved that H_2 production is optimum below the temperature. Compositions of CO were lower than 30 mol% due to the gasification producing more CO_2 in all cases. Water-gas-shift and methanation reactions were major reactions that took place in all studies, as observed in Table 17, whereby the yields of H_2 were always higher than CH_4.

Table 16. Composition of syngas from this study and from literature.

Optimized experimental conditions	Biomass feedstock	Syngas compositions (mol%)	Reference
Temperature =718.77°C, loading=0.3 g, ER=0.24.	*Nannochloropsis gaditana* LEA	H_2=36.35, CO=13.28, CO_2=23.28, CH_4=27.98.	This study
Temperature =766.79°C, loading=0.7 g, ER=0.1.	FEA	H_2=47.99, CO=26.05, CO_2=25.44, CH_4=11.08.	This study
Temperature =705.10°C, loading=1.44 g, ER=0.29, heating rate=22.24°C/min.	*Chorella vulgaris*	H_2=41.75, CO=18.63, CO_2=24.40, CH_4=15.19.	(Raheem, W. A. K. G., et al., 2015)
Temperature =500°C, loading=1.0 g, heating rate=30.0°C/min, gasifying agent=steam.	*Spirulina sp.*	H_2=21.1, CO=4.26, CO_2=36.2, CH_4=21.2.	(Onwudili et al., 2013)

3.3 Aspen Plus simulation

Simulation of the gasification model for LEA and FES was carried out in Aspen Plus using the same parameters as the gasification experiments. Figure 3 (a-b) and Figure 4 (a-b) display the comparison between the experimental optimization and Aspen Plus optimization plotted from the data in Table 17. The predicted H_2 and CO yields were higher than experimental H_2 yields for both LEA and FES, as observed in Figure 3 (a-b) and Figure 4 (a-b). The plots show the H_2 and CO compositions generated from 17 runs of gasification processes, as generated from the Design Expert software. The experimental and predicted data deviated away from each other. However, the trend of the changes in syngas compositions for all the 17 runs of the gasification process was similar for both experimental and predicted data.

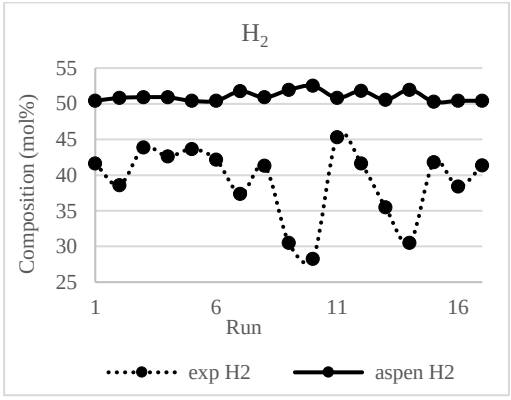

(a)

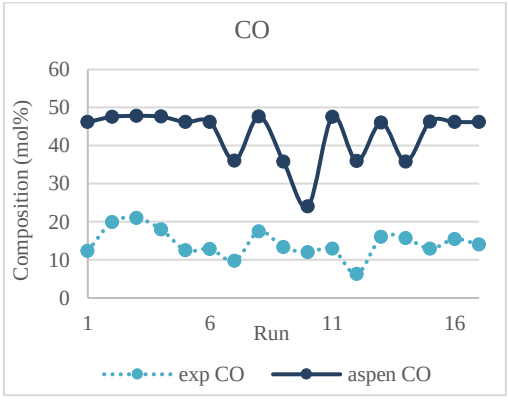

(b)

Figure 3. Compositions of syngas from experimental and Aspen Plus optimization for lipid extracted algae (LEA) (a) H_2 (b) CO**.**

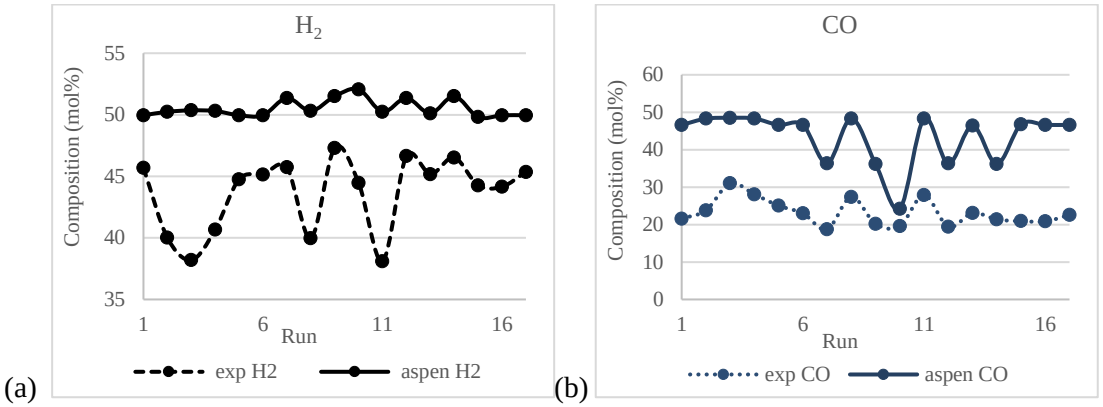

Figure 4. Compositions of syngas from experimental and Aspen Plus optimization for fucoidan extracted seaweeds (FEA) (a) H_2 (b) CO.

Table 17: Aspen Plus simulation data for LEA and FEA.

Run	Process parameters			Syngas compositions (mol %)			
				LEA		FEA	
	Temperature	Loading	ER	H_2	CO	H_2	CO
1.	800 (0)	0.5 (0)	0.3 (0)	50.41	46.18	49.96	46.61
2.	900 (+1)	0.6 (+1)	0.4 (+1)	50.82	47.57	50.24	48.29
3.	1000 (+2)	0.5 (0)	0.3 (0)	50.92	47.82	50.36	48.51
4.	900 (+1)	0.6 (+1)	0.2 (-1)	50.89	47.62	50.31	48.34
5.	800 (0)	0.3 (-2)	0.3 (0)	50.41	46.18	49.96	46.61
6.	800 (0)	0.7 (+2)	0.3 (0)	50.41	46.18	49.96	46.61
7.	700 (-1)	0.6 (+1)	0.4 (+1)	51.75	36.02	51.36	36.30
8.	900 (+1)	0.4 (-1)	0.2 (-1)	50.89	47.62	50.31	48.34
9.	700 (-1)	0.6 (+1)	0.2 (-1)	51.95	35.83	51.51	36.16
10	600 (-2)	0.5 (0)	0.3 (0)	52.50	23.99	52.07	24.23
11.	900 (+1)	0.4(-1)	0.4 (+1)	50.82	47.57	50.24	48.29
12.	700 (-1)	0.4 (-1)	0.4 (+1)	51.80	35.96	51.36	36.30
13.	800 (0)	0.5 (0)	0.1 (-2)	50.56	46.03	50.11	46.46
14.	700 (-1)	0.4 (-1)	0.4 (-1)	51.95	35.83	51.51	36.16
15.	800 (0)	0.5 (0)	0.5 (+2)	50.26	46.33	49.81	46.76
16.	800 (0)	0.5 (0)	0.3 (0)	50.41	46.18	49.96	46.61
17.	800 (0)	0.5 (0)	0.3 (0)	50.41	46.18	49.96	46.61

3.4 Data validation

Data validation for experimental optimization was done in Design Expert software, indicated by the R^2 values of all the plots higher than 0.75, denoting that the experimental data was valid and the polynomial model built was significant.

Figures 3 (a-b) and 4 (a-b) present the experimental gasification and simulation data from Aspen Plus, as represented by the solid line and dotted line, respectively. For H_2, the predicted syngas compositions were smaller in the range of values; meanwhile, experimental data displayed huge variations for each run, as displayed in Figure 3 (a) for LEA and Figure 4 (a) for FES. Nevertheless, the trend of the changes in syngas compositions from run 1 to run 17 was similar for all H_2 and CO yields from both algae residues, despite a few experimental data that trends were contradicted to the simulation data, for instance, run 10 for LEA and run 3 for FES. Figure 3 (a) shows that the experimental and

simulation H_2 yields from LEA exhibited a more similar trend compared to FES in Figure 4 (a). However, the deviation between experimental and simulation data was high, as represented by the RMSE values in Table 18.

Table 18. RMSE values for gasification runs.

Run	LEA	FEA
1.	24.72	20.39
2.	21.38	19.35
3.	19.62	15.08
4.	21.75	17.27
5.	24.28	18.66
6.	24.26	19.72
7.	21.18	16.65
8.	22.36	16.84
9.	21.99	18.23
10	19.13	18.39
11.	24.77	17.18
12.	22.17	18.37
13.	23.75	18.90
14.	20.81	17.02
15.	24.38	20.32
16.	23.32	21.37
17.	23.65	19.54

As for CO, FES showed better agreement between experimental and simulation data compared to LEA, as observed in Figure 4.13 (b). This can also be observed from the RMSE data from Table 19, where FES has lower RMSE values than LEA for all runs. Conversely, the deviations between both data were still large, as indicated by the RMSE values in Table 19. The higher the difference between the predicted and experimental data, the higher the RMSE values. All RMSE values were calculated for H_2 and CO yields, and it was found that the values for both algae residues fell out of the valid range of $0<RMSE<0.3$, hence, both experimental and simulation data were not in good agreement with each other. Hence, improvements of the experimental gasification setup, for instance, proper insulation of the gasifier set up to minimize heat loss that caused the actual gasification temperature to be lower than the set temperature must be carried out to improve the syngas composition. The large deviations also originated from the limitations of the Aspen Plus gasification simulation, where the duration of the gasification was excluded and caused the difference in the syngas composition from the experiments and the Aspen Plus simulation.

3.5 Gasification efficiency

The study of gasification efficiency yielded carbon conversion efficiency (CCE), as displayed in Table 19 below. CCE is defined as the ratio of carbon converted into gaseous products to the carbon contained in the LEA and FES on a dry mass basis (Katsaros et al., 2019). The syngas compositions taken into account were the carbon-containing gases, CO, CO_2, and CH_4. Gasification results showed that LEA produced a higher H_2 yield than FES, whereby vice versa for CO and other carbon-containing gases; CO_2 and CH_4. FES showed a higher average CCE, 80.42%, compared to LEA, which had 66.36% of CCE, where more carbon in FES was converted into CO, CO_2, and CH_4 than LEA. From the proximate analysis section, LEA possessed lower oxygen content compared to FES. High CCE was also associated with the high oxygen content in the FES, whereby more oxygen was available to react with volatiles

and tar to produce CO and CO_2 (Katsaros et al., 2019). This led to the lower H_2 yield from FES compared to LEA.

Table 19. CCE for gasification of LEA and FEA.

Run	LEA				Seaweeds			
	Syngas compositions (mol %)			CCE (%)	Syngas compositions (mol %)			CCE (%)
	CO	CO_2	CH_4		CO	CO_2	CH_4	
1.	12.34	18.11	27.91	64.87	21.56	16.52	19.25	72.25
2.	19.92	15.96	24.24	64.67	23.81	14.62	12.55	65.80
3.	20.98	12.57	23.00	61.75	31.00	15.60	15.21	87.65
4.	18.00	15.43	23.96	62.23	28.08	15.98	14.28	80.09
5.	12.52	18.42	25.42	61.31	25.04	19.03	17.17	87.05
6.	12.89	17.50	27.49	64.34	22.98	21.74	20.12	86.32
7.	9.75	22.42	30.48	69.00	18.69	25.44	16.14	79.92
8.	17.48	15.57	25.64	64.47	27.39	18.14	10.51	75.86
9.	13.31	21.13	32.05	73.90	20.15	23.66	19.88	91.95
10	12.01	25.74	34.00	**78.41**	19.60	25.18	28.74	**95.31**
11.	12.97	16.19	25.52	60.61	27.86	17.94	17.10	90.57
12.	6.30	22.24	29.84	64.83	19.38	22.10	21.98	89.17
13.	16.02	19.93	26.57	67.09	23.07	15.78	12.11	64.46
14.	15.67	23.25	30.58	74.92	21.36	18.07	18.04	82.19
15.	12.91	18.60	26.72	63.79	20.91	18.83	15.00	72.92
16.	15.48	15.98	28.18	66.87	20.85	17.60	15.39	72.65
17.	13.99	17.31	27.35	65.01	22.56	16.75	19.33	74.51
Average				**66.36**				**80.42**

For both algae residues, the highest CCE values of 78.41 and 95.31% were obtained for run 10 for LEA and FES, respectively, conducted at 600℃, loading 0.5 g and ER of 0.3. This was ascribed with the boosted production of CO_2 and CH_4 at a lower temperature due to the effect of water-gas shift (WGS) reaction ($CO+H_2O \leftrightarrow CO_2+H_2$) that was exothermic and Bouduard reaction ($C+CO_2 \rightarrow 2CO$) that was endothermic. Both WGS and Bouduard reactions suppressed the production of CO_2 at the higher temperature; however, Bouduard reaction promoted CO production as the temperature went higher. Cherad et al. (2014) also reported that production of CH_4 was also lower at higher temperatures due to the heat of CH_4 formation that was exothermic. Lu & Savage (2015) discussed that the highest energy recovery was obtained at low-temperature gasification of *Nannochloropsis sp*. biomass at 600℃.

As for ER value, the mechanisms of WGS and Bouduard reactions have revealed that higher oxygen content promoted CO_2 production. Hence, higher concentrations of CO and H_2O as the reactants of the reactions resulted in boosted production of CO_2. Different results were obtained from Karthik Ramakrishnan & Yang (2014) that reported that increasing ER value from 0.21 to 0.3 resulted in decreased CO, CO_2, and CH_4 yields. Biomass loading did not significantly affect the syngas compositions as it did not directly involve the gasification reaction mechanisms. However, the yields of CO, CO_2, and CH_4 were increased as the *Chlorella vulgaris* biomass was increased from 1g (Raheem, W. A. K. G., et al., 2015). Cherad et al. also observed the same phenomenon from the gasification of macroalgae *Laminaria hyperborean* as the loading was doubled from the initial loading value.

4. Conclusion

The effect of different process parameters for high syngas production was experimentally and theoretically evaluated. The effects of process parameters on syngas compositions were most significant for temperature, followed by ER, and least significant for loading. Experimental optimization was

successfully done in Central Composite Design (CCD) approach, producing a good prediction of H_2 and CO yields based on the input process parameters. The optimized conditions were found at 718.77℃, 0.3 g loading, and ER of 0.24, producing 36.38 and 13.28 mol% of H_2 and CO, respectively for LEA and 766.79℃, 0.7 g loading and ER of 0.1 that produced 47.99 and 26.05 mol% of H_2 and CO, respectively for FES. Aspen Plus simulation results showed poor agreement with the experimental syngas compositions; however, both optimization studies showed similar changes in syngas composition for all runs. The RMSE values were too high for both LEA and FES; hence, improvements in the experimental and simulation of the gasification needed to be performed to obtain a good agreement between these two gasification approaches.

References

[1] aspentech. (2013). *Getting Started Modeling Processes with Solids*. Aspen Technology, Inc. www.aspentech.com
[2] Bowyer, J., Howe, J., Levins, R. A., Groot, H., Fernholz, K., Pepke, E., & Henderson, C. (2018). Third Generation Biofuels: Implications for Wood-Derived. In *Dovetail Partners, Inc.* (Issue February).
[3] Chen M, Liu T, Chen X, Chen L, Zhang W, Wang J, et al. 2012 Subcritical co-solvents extraction of lipid from wet microalgae pastes of Nannochloropsis sp *Eur J Lipid Sci Technol* **114** 205 - 12.
[4] Chen W-H, Lin B-J, Huang M-Y, Chang J-S. 2015 Thermochemical conversion of microalgal biomass into biofuels: A review *Bioresour Technol* **184** 314-27.
[5] Chen W-H, Hsieh T-C, Jiang TL. 2008 An experimental study on carbon monoxide conversion and hydrogen generation from water gas shift reaction *Energy Convers Manage* **49**(10) 2801-8.
[6] Cherad R, Onwudili JA, Williams PT, Ross AB. 2014 A parametric study on supercritical water gasification of Laminaria hyperborea: A carbohydrate-rich macroalga *Bioresour Technol* **169** 573-80.
[7] ohce MK, Rosen MA, Dincer I. 2011 Efficiency evaluation of a biomass gasification-based hydrogen production *Int J Hydrogen Energy* **36**(17) 11388-98.
[8] Doherty W, Reynolds A, Kennedy D. 2009 The effect of air preheating in a biomass CFB gasifier using ASPEN Plus simulation *Biomass Bioenergy* **33**(9) 1158-67.
[9] Ebadi AG, Hisoriev H, Zarnegar M, Ahmadi H. 2019 Hydrogen and syngas production by catalytic gasification of algal biomass (Cladophora glomerata L.) using alkali and alkaline-earth metals compounds *Environ Technol* **40**(9) 1178-84.
[10] Karthik Ramakrishnan, & Yang, W. (2014). *Optimization and Process modelling of Municipal Solid Waste using Plasma Gasification for Power Generation in Trichy, India.* KTH Royal Institute of Technology.
[11] Katsaros G, Shankar Pandey D, Horvat A, Tassou S. 2019 Low temperature gasification of poultry litter in a lab-scale fluidized reactor *Energy Procedia* **161** 57-65.
[12] Sanchez-Silva L, López-González D, Garcia-Minguillan AM, Valverde JL. 2013 Pyrolysis, combustion and gasification characteristics of Nannochloropsis gaditana microalgae *Bioresour Technol* **130** 321-31.
[13] Lfatinský P, Palit A. 2016 Wood Pyrolysis Using Aspen Plus Simulation and Industrially Applicable Model *GeoScience Engineering* **62** 11 - 6.
[14] Lu Y, Savage PE. 2015 Supercritical water gasification of lipid-extracted hydrochar to recover energy and nutrients *The Journal of Supercritical Fluids* **99** 88-94.
[15] Maurya R, Chokshi K, Ghosh T, Trivedi K, Pancha I, Kubavat D, et al. 2016 Lipid Extracted Microalgal Biomass Residue as a Fertilizer Substitute for Zea mays L *Frontiers in Plant Science* **6** 1266.
[16] Meillisa A, Siahaan EA, Park J-N, Woo H-C, Chun B-S. 2013 Effect of subcritical water hydrolysate in the brown seaweed Saccharina japonica as a potential antibacterial agent on food-borne pathogens *J Appl Phycol* **25**(3) 763-9.
[17] Mutlu ÖÇ, Zeng T. 2020 Challenges and Opportunities of Modeling Biomass Gasification in Aspen

Plus: A Review *Chemical Engineering & Technology* **43**(9) 1674-89.
[18] Nurdiawati A, Zaini IN, Aziz M. 2018 Efficient hydrogen production from algae and its conversion to methylcyclohexane *Chemical Engineering Transactions* **70** 1507-12.
[19] Onwudili JA, Lea-Langton AR, Ross AB, Williams PT. 2013 Catalytic hydrothermal gasification of algae for hydrogen production: Composition of reaction products and potential for nutrient recycling *Bioresour Technol* **127** 72-80.
[20] Panda, C. (2012). *Aspen Plus Simulation Studies on Biomass and Experimental Gasification*.
[21] Maity JP, Bundschuh J, Chen C-Y, Bhattacharya P. 2014 Microalgae for third generation biofuel production, mitigation of greenhouse gas emissions and wastewater treatment: Present and future perspectives – A mini review *Energy* **78** 104-13.
[22] Raheem A, Ji G, Memon A, Sivasangar S, Wang W, Zhao M, et al. 2018 Catalytic gasification of algal biomass for hydrogen-rich gas production: Parametric optimization via central composite design *Energy Convers Manage* **158** 235-45
[23] Raheem A, Sivasangar S, Wan Azlina WAKG, Taufiq Yap YH, Danquah MK, Harun R. 2015 Thermogravimetric study of Chlorella vulgaris for syngas production *Algal Research* **12** 52-9.
[24] Raheem A, W. A. K. G WA, Taufiq Yap YH, Danquah MK, Harun R. 2015 Optimization of the microalgae Chlorella vulgaris for syngas production using central composite design *RSC Advances* **5**(88) 71805-15.
[25] Ranjith Kumar R, Hanumantha Rao P, Arumugam M. 2015 Lipid Extraction Methods from Microalgae: A Comprehensive Review *Frontiers in Energy Research* **2** 1-9.
[26] Roh M-K, Uddin MS, Chun B-S. 2008 Extraction of fucoxanthin and polyphenol from Undaria pinnatifida using supercritical carbon dioxide with co-solvent *Biotechnology and Bioprocess Engineering* **13**(6) 724-9.
[27] Rosha P, Kumar S, Vikram S, Ibrahim H, Al-Muhtaseb AaH. 2021 H2-enriched gaseous fuel production via co-gasification of an algae-plastic waste mixture using Aspen PLUS *Int J Hydrogen Energy*.
[28] Sun, K. (2014). *Optimization of biomass gasification reactor using Aspen Plus*. Telemark University College.
[29] Veerasamy R, Rajak H, Jain A, Sivadasan S, Christapher PV, Agrawal R. 2011 Validation of QSAR Models - Strategies and Importance *Int J Drug Design and Discov* **2** 511-9.